Biosensors and Bioelectronics 62 (2014) 113–119

Contents lists available at ScienceDirect

Biosensors and Bioelectronics

journal homepage: www.elsevier.com/locate/bios

Gold nanoparticle supported phospholipid membranes as a biomimetic biosensor platform for phosphoinositide signaling detection

Qian Wen, Si-Jia Liu, Li-Juan Tang*, Ying Tang, Jian-Hui Jiang*

State Key Laboratory of Chemo/Bio-Sensing and Chemometrics, College of Chemistry and Chemical Engineering, Hunan University, Changsha 410082, PR China

ARTICLE INFO

Article history:
Received 6 May 2014
Received in revised form
9 June 2014
Accepted 10 June 2014
Available online 12 June 2014

Keywords:
Biosensor
Gold nanoparticles
Phospholipid membranes
Phosphoinositide signaling
Colorimetric detection

ABSTRACT

Enzyme mediated phosphoinositide signaling plays important regulatory roles in diverse cellular processes and has close implication in human diseases. However, detection of phosphoinositide enzymes remains a challenge because of the difficulty in discriminating the phosphorylation patterns of phosphoinositide. Here we develop a novel enzyme-activated gold nanoparticles (AuNPs) assembly strategy as a homogeneous colorimetric biosensor for activity detection of phosphoinositide kinases and phosphatases. This strategy utilizes a biomimetic mechanism of phosphoinositide signaling, in which AuNP supported phospholipid membranes are constructed to mimic the cellular membrane substrate, and AuNPs modified with the pleckstrin homology (PH) domain of cytosolic proteins are designed for specific, multivalent recognition of phosphorylated phosphoinositides. This biomimetic strategy enables efficient enzymatic reactions of the substrate and highly selective detection of target enzyme. The biosensor is demonstrated for the detection of phosphoinositide 3-kinase (PI3K) and phosphatase with tensin homology (PTEN). The results revealed that it allows sensitive, rapid visual detection of the enzymes with pM detection limits and four-decade wide dynamic ranges, and is capable of detecting enzyme activities in complex cell lysate samples. This biosensor might provide a general biosensor platform for high-throughput detection of phosphoinositide enzymes with high sensitivity and selectivity in biomedical research and clinical diagnostics.

1. Introduction

A phosphoinositide signaling system, regulated by reversible phosphorylation of the inositol headgroup by phosphoinositide kinases and phosphatases (Bartel, 2004), plays important roles in diverse fundamental cellular processes (Bunney and Katan, 2010). Dysfunction of these enzymes is known to have close implication in tumors, diabetes and other diseases (Wymann and Schneiter, 2008). Robust detection of the phosphoinositide enzymes represents a significant approach to understanding the molecular mechanisms and developing theranostic tools. Activity assay of phosphoinositide enzymes is typically performed by monitoring the transfer of phosphate from or to phosphoinositides using radiometric methods (Knight et al., 2007; Taniguchi et al., 2006). Fluorescence based techniques such as fluorescence resonance energy transfer have recently attracted great interest in such assays (Wei et al., 2013; Yuan et al., 2009; Tzenaki et al., 2012). These techniques, however, have a limitation in requiring fluorescence labels for phosphoinositides and their binding proteins or a hazardous radioactive co-substrate. They also show limited sensitivity and dynamic ranges because of the use of competitive assay format.

Phospholipids can provide a biocompatible coating for various nanomaterials including carbon nanotubes, graphene, silica nanoparticles, and luminescent quantum dots or upconversion nanoparticles (Nie et al., 2009; Liu et al., 2012; Wang et al., 2010; Zheng et al., 2014; Li et al., 2012a). The phospholipid-coated gold nanoparticles (AuNPs) have also been successful synthesized as an efficient carrier for drug delivery (Pornpattananangkul et al., 2011), or as a sensitive label for surface enhanced Raman scattering detection (Qian et al., 2008). Nevertheless, the use of phospholipid-coated AuNPs for colorimetric biosensors, to our knowledge, has not been reported. It is known that assembly of AuNPs can generate strong plasmonic coupling between adjacent

* Corresponding authors. Tel./fax: +86 731 88821916.
E-mail addresses: tanglijuan@hnu.edu.cn (L.-J. Tang), jianhuijiang@hnu.edu.cn (J.-H. Jiang).

http://dx.doi.org/10.1016/j.bios.2014.06.016
0956-5663/

nanoparticles with a concomitant visual color change (Saha et al., 2012; Giljohann et al., 2010). This creates a useful platform for developing colorimetric biosensor for different targets such as DNA (Zhang et al., 2012), proteins (Li et al., 2012b), small molecules (Chen et al., 2014), and metal ions (Guo et al., 2011). Because of the vast versatility and the high performance of this platform, it is expected that phospholipid-coated AuNPs can also be used for the development of a sensitive and convenient colorimetric biosensor for phosphoinositide signaling detection.

Herein we report a novel homogeneous colorimetric biosensor strategy for activity detection of phosphoinositide kinases and phosphatases, for the first time, based on enzyme-activated assembly of phospholipid-coated AuNPs or AuNP supported phospholipid membranes. This strategy relies on a biomimetic mechanism of phosphoinositide signaling that is achieved via binding of their enzyme-modified head groups to the pleckstrin homology (PH) domain of cytosolic proteins or cytosolic domains of membrane proteins (Lemmon, 2008; Bethoney et al., 2009). A cellular-membrane-mimicking nanostructure is designed using AuNP supported phospholipid membranes, in which the phosphoinositides are incorporated. The supported phospholipid membranes provide a biomimetic substrate enabling efficient enzymatic reactions on the surfaces. To directly transduce the enzymatic reactions, AuNPs decorated with PH domains of phosphoinositide-binding proteins are constructed to mimic a specific, multivalent biological receptor of the enzymatically modified phosphoinositides. In the presence of target phosphoinositide modification, the AuNP supported phospholipid membranes can form cross-linked assembly with the AuNPs decorated with PH domains, delivering a visual signal because of the plasmonic coupling of AuNPs (Saha et al., 2012; Giljohann et al., 2010). Hence, the developed biosensor strategy can be configured into a potentially high-throughput homogeneous format that allows sensitive, rapid, and convenient colorimetric detection of phosphoinositide enzymes without the need of particular labeling reagents. To demonstrate the feasibility of this strategy, we choose phosphoinositide 3-kinase (PI3K) and phosphatase with tensin homology (PTEN) as the model systems. PI3K and PTEN are phosphoinositide-modifying enzymes among the most frequently mutated proteins in cancer. These two enzymes reversibly regulate the levels of phosphatidylinositol-3,4,5-trisphosphate (PtdIns(3,4,5)P3) and have attracted the most interest in phosphoinositide signaling researches (Cantley, 2002; Cully et al., 2006).

2. Experimental

2.1. Reagents and apparatus

Phosphatidylinositol 4,5-bisphosphate (PIP2), phosphatidylinositol-3,4, 5-trisphosphate (PIP3), 1,2-dimyristoyl-sn-glycero-3-phosphocholine (DMPC) and 1-myristoyl-2-hydroxy-snglycero-3-phosphocholine (MHPC) were purchased from Avanti Polar Lipids (Alabaster, USA). Phosphoinositide 3 kinase (PI3K) was obtained from US Biological (Swampscott, USA). PIP3 binding PH domain and phosphatase with tensin homology (PTEN) were from Cayman Chemical Company (Michigan, USA). PI3K inhibitor LY294002 (Martelli et al., 2006) and PTEN inhibitor SF1670 (Li et al., 2011) were purchased from Selleckchem (Houston, USA). The three human cancer cell lines (MCF-7, Hela and MDA-MB-231) were purchased from XiangYa Central Experiment Laboratory (Changsha, China). PI3K activity was evaluated with a PI3 kinase ELISA kit (Echelon Biosciences, K-1000s). Trisodium citrate, $HAuCl_4 \cdot 3H_2O$, ascorbic acid, bovine serum and albumin (BSA) were from Sigma-Aldrich (Missouri, USA). All other chemicals were of analytical grade and obtained from Sinopharm Chemical Reagent Co. Ltd. (Shanghai, China). All solutions were prepared using ultrapure water, which was obtained through a Millipore Milli-Q water purification system (Billerica, MA, USA) and had an electric resistance > 18.3 MΩ.

2.2. Preparation of phospholipid-coated AuNPs

Phospholipid-coated AuNPs were synthesized according to a modified procedure for the liposome synthesis. A mixture of DMPC, MHPC and PIP2 or PIP3 (6 M:6 M:0.1 M) was prepared using 3 mL 6:1 chloroform/methanol as a solvent in a flask (Tam et al., 2012). Slowing evaporation of the mixture using a rotating apparatus at 20 °C enabled the formation of a phospholipid bilayer on the inner wall of the flask. Then, AuNPs (1 mL, 8 nM) were added to the flask and stirred followed by gradual heating up to 50 °C. The mixture was allowed to continue swelling for 1 h to obtain the synthesized phospholipid-coated AuNPs. Purification of the phospholipid-coated AuNPs was achieved through three rounds of centrifugation at 30,000*g* for 15 min and re-suspending the sediments in 1 mL phosphate buffer (PB, 0.1 mM, pH 7.4) to sufficiently remove all excessive free liposomes or lipids. The obtained phospholipid-coated AuNPs, with PIP2 or PIP3 incorporated in the membranes, were suspended in 1 mL PB (0.1 mM, pH 7.4) containing 1 μM BSA and stored at 4 °C for future use. The final concentration of the phospholipid-coated AuNPs was ~8 nM, assuming that the loss of AuNPs could be overlooked during the preparation process.

2.3. Preparation of PIP3 binding PH domain modified AuNPs

PIP3 binding PH domain modified AuNPs were prepared according to the following procedure. Briefly, 10 μL solution containing 25 μg PIP3 binding PH domain was added dropwise (~1 μL each drop) into 300 μL 8 nM AuNPs in PB (0.1 mM, pH 8.0) under stirring for 30 min followed by aging for overnight at 4 °C. Excessive PIP3 binding PH domain was removed via centrifugation at 20,000*g* for 5 min followed by re-suspending the sediment in 1 mL ultrapure water. These steps were repeated twice to sufficiently remove all excessive proteins. The obtained PIP3 binding PH domain modified AuNPs were suspended in 1 mL 1 μM BSA solution and stored at 4 °C for future use. The final concentration of PIP3 binding PH domain modified AuNPs was ~8 nM, assuming that the loss of AuNPs could be neglected during the preparation process. For the preparation of BSA modified AuNPs, we used the same procedures by replacing PIP3 binding PH domain by BSA.

2.4. Activity assay of PI3K

In a 20 μL aliquot of 4 nM PIP3-incorporated phospholipids-coated AuNPs solution, 2.5 μL PI3K solution of varying concentrations (final concentration ranging from 0 to 50 nM) containing Tris–HCl buffer (40 mM Tris–HCl, 100 μM ATP, 20 mM $MgCl_2$, pH 7.5) was added. The mixture was incubated at 30 °C for 10 min. Then, 10 μL 8 nM PIP3 binding PH domain modified AuNPs were added to the mixture. The resulting mixture was incubated at 30 °C for 10 min followed by spectral measurements and other characterization. Samples were diluted 2-fold in water just prior to analysis.

2.5. Activity assay of PTEN

In a 20 μL 4 nM PIP3-incorporated phospholipids-coated AuNPs solution, 2.5 μL PTEN solution of varying concentrations (final concentration ranging from 0 to 18 nM) containing reaction buffer (25 mM Tris–HCl, 140 mM NaCl and 2.7 Mm KCl, 10 mM DTT, pH 7.4) was added. The mixture was incubated at 30 °C for 10 min

followed by the addition of 10 μL 8 nM PIP3 binding PH domain modified AuNPs. The resulting mixture was incubated at 30 °C for 10 min followed by spectral measurements and other characterization. Samples were diluted 2-fold in water just prior to analysis.

3. Results and discussion

3.1. Design of phospholipid-coated AuNPs as a biomimetic biosensor for phosphoinositide signaling detection

Scheme 1 illustrates the principle of the colorimetric biosensor for PI3K based on enzyme-activated assembly of AuNP supported phospholipid membranes and AuNP labeled binding PH domains. PI3K catalyzes the phosphorylation of the D-3 position of the inositol ring in PIP2 to yield PIP3 in the presence of the co-substrate ATP (Scheme 2). To construct the colorimetric sensor, we utilize the inherent amphiphilic property of phospholipids and their ability to self-assemble into organized structures. It is demonstrated that various phospholipids can be self-assembled as a membrane on the AuNPs' surfaces (Thaxton et al., 2009; Tam et al., 2010). This motivated us to engineer an artificial cell membrane by using such AuNP supported phospholipid membranes to mimic the cellular surrounding for enzymatic reactions (Scheme 1A). The supported phospholipid membranes consisted of three phospholipids components including DMPC, MHPC and the substrate PIP2. The use of MHPC was necessary for the assembly of phospholipid membranes on AuNP. It was reported that a mix of single and double-chain phospholipids was likely to generate a tighter curvature and result in closer interaction of positively-charged choline headgroups with negatively-charged AuNP surfaces (Tam et al., 2010). The substrate phosphoinositide PIP2 were incorporated in the phospholipid membrane via hydrophobic interaction, while exposing their hydrophilic head groups outside the membrane for enzymatic reactions. After constructing the AuNP supported phospholipid membranes and the AuNPs modified with the PH domains specifically binding to PIP3, the colorimetric assay of PI3K activity could be performed immediately (Scheme 1B). In the presence of kinase PI3K and ATP, the substrate PIP2 anchored onto the AuNP supported phospholipid membranes was phosphorylated and converted into PIP3. The phosphorylated product PIP3 could then specifically bind to the PH domains decorated on the AuNPs, triggering a cross-linked assembly of the phospholipid membrane-coated AuNPs with the PH domain-modified AuNPs. This assembly delivered a colorimetric signal that was quantitatively correlated to PI3K activity. In contrast, in the case when there was no PI3K activity in the system, no PIP3 was produced on the AuNP supported phospholipid membranes, which could not bind to the PH domains

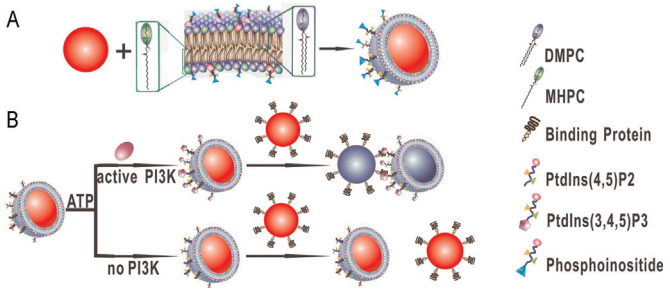

Scheme 1. Illustration of the biosensor strategy for PI3K. (A) Synthesis of AuNP supported PIP2-incorporated phospholipid membranes; (B) PI3K assay via enzymatic activated assembly of AuNP supported phospholipid membranes with PIP3 binding PH domain modified AuNPs.

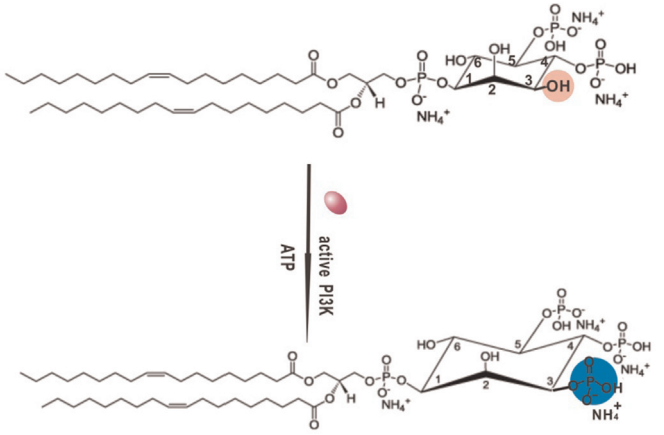

Scheme 2. Illustration of PI3K catalyzes the phosphorylation of the D-3 position of the inositol ring in PIP2 to yield PIP3 in the presence of the co-substrate ATP.

decorated on AuNPs, and thus no colorimetric change would be obtained.

3.2. Enzyme-activated Colorimetric Biosensing Strategy for PI3K assay

Fig. 1A depicts typical absorption spectra responses obtained in biosensor construction and PI3K assay. The AuNP supported phospholipid membranes were prepared readily according to a modified procedure for the liposome synthesis (Hill and Mirkin, 2006; Tam et al., 2012). The citrate-protected AuNPs were well dispersed in aqueous solution, displaying a red color with a single surface plasmon absorption peak centered at 522 nm (Fig. 1A, curve a). After decorated with phospholipid membranes, AuNPs exhibited a slight red-shift of the absorption peak to 526 nm (Fig. 1A, curve b), which implied a surface chemistry changed of AuNPs (Ip et al., 2011) and evidenced a close decoration of the phospholipid membranes on AuNPs. Subsequent reactions of the AuNP supported phospholipid membranes with 50 nM PI3K for 10 min did not cause an appreciable change of the absorption spectrum (Fig. 1A, curve c), implying that the enzymatic modification had little effect on the stability and the surface chemistry of the AuNPs. After AuNPs modified with the PIP3-specific PH domains added, the solution showed a rapid color fading and became almost colorless in 10 min with the absorption peak decreased by ~78% (Fig. 1A, curve e), a typical response of the network-like assembly of AuNPs (Saha et al., 2012; Giljohann et al., 2010). In contrast, with the PH domain modified AuNPs added in the solution containing phospholipid membranes coated AuNPs without the addition of PI3K, the solution remained a red color and merely showed a slight intensity change due to the mixing of two solutions (Fig. 1A, curve d). Compared the latest two experiments, we could infer that the formation of cross-linked assembly of the PH domain-modified AuNPs with the phospholipid membrane-coated AuNPs was originated from PI3K. Based on the high specificity of the PH domain against PIP3, we then concluded that PI3K mediated efficient phosphorylation of PIP2 into PIP3 on the AuNP supported phospholipid membranes.

To further confirm the decorated of AuNPs with phospholipids and the PI3K-mediated reaction, electrospray ionization mass spectrometry (ESI-MS) was used in the positive ion mode for directly analyzing the organic compounds coated on the AuNPs (Fig. 1B). For the freshly-prepared AuNPs obtained by the citrate-reduction method, we do not obtain any characteristic mass peak of phospholipids (Fig. 1B, a). But, for AuNPs coated with phospholipid membranes, three remarkable ion peaks (468.2617, 678.4712, and 1075.4055 Da) were obtained (Fig. 1B, b), which could be

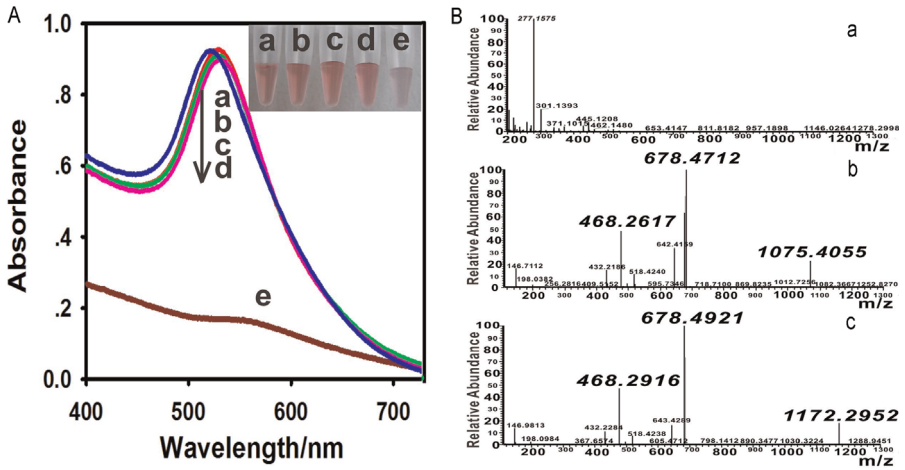

Fig. 1. (A) Typical absorption spectral responses obtained in phospholipid-coated AuNPs synthesis and PI3K assay. (a) Citrate-protected AuNPs; (b) PIP2-incorporated phospholipid-coated AuNPs; (c) PIP2-incorporated phospholipid-coated AuNPs reacting with 50 nM PI3K; (d) PIP2-incorporated phospholipid-coated AuNPs mixed with PH domain modified AuNPs; (e) PIP2-incorporated phospholipids-coated AuNPs reacting with 50 nM PI3K followed by addition of PH domain modified AuNPs. Inset: photograph of the corresponding solutions. (B) ESI-MS spectra obtained from (a) citrate-protected AuNPs; (b) PIP2-incorporated phospholipid-coated AuNPs; (c) PIP2-incorporated phospholipid-coated AuNPs reacting with PI3K. (For interpretation of the references to color in this figure, the reader is referred to the web version of this article.)

ascribed to the mother ions of $[MHPC\ H]^+$, $[DMPC\ H]^+$ and $[PIP2\ 3NH4\ H]^+$ (calculated 468.278, 678.640, and 1075.461 Da). These data gave clear evidence for the successful decoration of AuNPs with phospholipid membranes. After the AuNPs supported phospholipid membranes reacting with PI3K, a new mass peak appeared at 1172.2952 Da accompanying with a diminished peak at 1075.4055 Da (Fig. 1B, c). This observation implied a high-yield conversion of PIP2 into PIP3 (calculated 1172.169 Da), verifying the effectiveness of PI3K-mediated reaction on the AuNP supported phospholipid membranes. The synthesis of the AuNPs coated with phospholipid membranes and the formation of cross-linked AuNPs aggregates were further verified by dynamic light scattering (DLS) (Fig. S1). The citrate-protected AuNPs gave an average hydrodynamic diameter of ~32 nm, while the AuNPs coated with phospholipids membranes gave an average hydrodynamic diameter of ~48 nm. After the phospholipid-coated AuNPs reacting with 50 nM PI3K, the average hydrodynamic diameter displayed a slight increase to ~53 nm. After the addition of the PH domain-modified AuNPs, a substantial increase in the average hydrodynamic diameter (~1238 nm) was observed, suggesting the assembly of the AuNPs into large aggregates.

In addition, as revealed by transmission electron microscopy (TEM) images, the citrate-protected AuNPs, the phospholipid-coated AuNPs, and the mixture of the phospholipid-coated AuNPs and the PH domain-modified AuNPs were all well monodispersed (Fig. 2a–c). Large aggregates was only obtained in the case where the phospholipid-coated AuNPs were firstly subjected to the reaction with PI3K followed by the addition of the PH domain-modified AuNPs (Fig. 2d). These DLS and TEM data were in good consistence with those obtained with the absorption spectral measurements, testifying the successful modifications of the AuNPs and the assembly of AuNPs into large aggregates in response to PI3K signaling.

Further control experiments were performed to verify that the assembly of AuNPs was specific to PI3K signaling, as shown in Fig. 3. In the control where the substrate PIP2 was not incorporated in the AuNP supported phospholipids membranes, no appreciable spectral variation was obtained after the reaction of the phospholipids membranes with PI3K followed in the presence of ATP by adding the PH domain modified AuNPs (Fig. 3, curve a). This control implied that the reaction of substrate PIP2 with PI3K was necessary for the assembly of AuNPs in our assay.

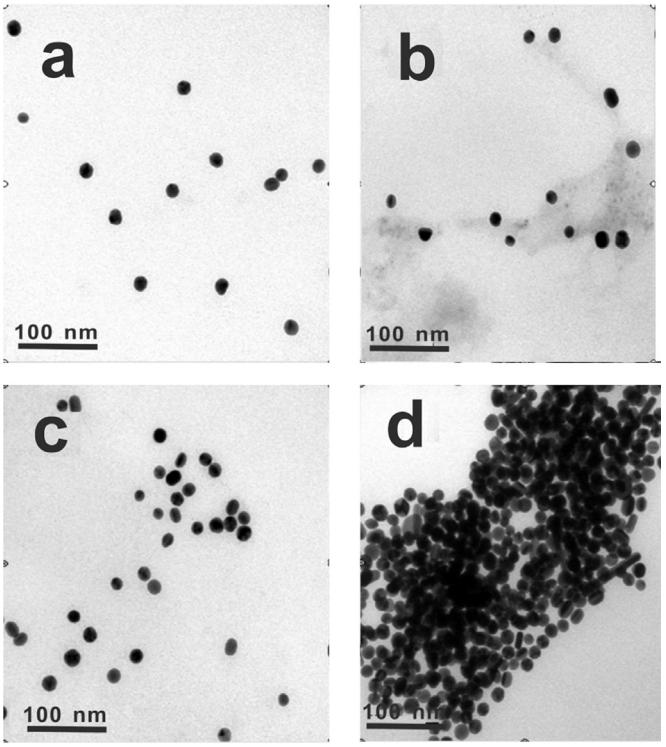

Fig. 2. TEM images in the synthesis of AuNPs coated with phospholipid membranes and in the assay of PI3K. (a) Citrate-protected AuNPs; (b) PIP2-incorporated phospholipid-coated AuNPs; (c) PIP2-incorporated phospholipid-coated AuNPs mixed with PH domain modified AuNPs; (d) PIP2-incorporated phospholipids-coated AuNPs reacting with 50 nM PI3K followed by addition of PH domain modified AuNPs.

Alternatively, after the AuNP supported phospholipids membranes reacted with PI3K in the presence of ATP, there was also no positive colorimetric response to the addition in the reaction mixture with bovine serum albumin (BSA) modified AuNPs rather than the PH domain modified AuNPs (Fig. 3, curve b). This control evidenced that the assembly of AuNPs in our assay specifically arose from the interaction between the PH domain and the product PIP3 from the kinase reaction. Additionally, we performed control experiments in which the PIP2-incorporated phospholipid-

coated AuNPs was incubated with PI3K in the presence of its inhibitor LY294002 (100 μM) or in the absence of the co-substrate ATP followed by the addition of the PH domain modified AuNPs. As anticipated, no remarkable color change was observed in the case where ATP was absent (Fig. 3, curve c). Only a slight decrease of the absorption peak was obtained for the case when the PI3K inhibitor was included in the kinase reaction, which was attributed to incomplete inhibition of the PI3K activity in the presence of 100 μM LY294002 (Fig. 3, curve d). The observations from these two controls suggested that an active reaction of PI3K was required for the assembly of AuNPs. To further validate that the assembly of AuNPs was specific to the interaction between the phosphorylated product PIP3 and the PH domain modified AuNPs, we prepared AuNP supported phospholipids membranes incorporating PIP3 instead of PIP2. After the PH domain modified AuNPs added, the supported phospholipids membranes solution displayed a rapid color fading and turned almost colorless (Fig. 3, curve e). This observation clearly manifested that the specific interaction between PIP3 and its binding PH domain was the driving force for the assembly of AuNPs in our assay. Taking together, the colorimetric responses in our assay were highly specific to the PI3K-catalyzed phosphorylation of PIP2 into PIP3, implying our biosensing strategy provided a highly selective and visual analytical platform for detection of PI3K signaling.

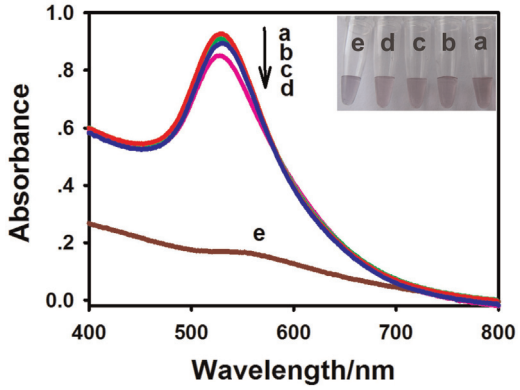

Fig. 3. Absorption spectral responses of the biosensor in the assay of PI3K. (a) PIP2-free phospholipid-coated AuNPs + 50 nM PI3K + ATP + PH domain modified AuNPs; (b) PIP2-incorporated phospholipid-coated AuNPs + 50 nM PI3K + ATP + BSA-modified AuNPs; (c) PIP2-incorporated phospholipid-coated AuNPs + 50 nM PI3K + PH domain modified AuNPs; (d) PIP2-incorporated phospholipid-coated AuNPs + 50 nM PI3K + ATP + inhibitor LY294002 (100 μM) + PH domain modified AuNPs; (e) PIP3-incorporated phospholipid-coated AuNPs + PH domain modified AuNPs. Inset: photograph of the corresponding solutions.

3.3. Quantitative activity screening of PI3K using the Biosensing Strategy

The ability of the Biosensing Strategy for quantitative activity screening of PI3K was then investigated. A series of samples containing the PI3K of different concentrations were incubated with the phospholipid-coated AuNPs followed by the addition of the PH domain modified AuNPs. Fig. 4 displays the corresponding absorption spectral responses in the assays. It was observed that the red color of the reaction mixtures was gradually attenuated with increasing PI3K concentration, suggesting that the AuNPs were assembled into larger aggregates in greater extent in the presence of higher PI3K concentration. These visual observations were consistent with the absorption spectral measurements. Actually, the absorption peaks were found to show gradual decrease with increasing PI3K concentration with a slight concomitant red-shift from 526 nm to 560 nm. A plot of the absorbance readings at 526 nm versus the PI3K concentrations revealed a dynamic correlation between the peak absorbances and the PI3K concentrations in the range from 5 pM to 50 nM. A linear correlation was obtained for the peak responses versus the logarithmic PI3K concentrations over the four-decade range with a detection limit of 1 pM, implying a wide linear range and high sensitivity of this biosensor (Fig. S2). This detection limit was over 10-fold better than existing methods for PI3K assays (Wei et al., 2013; Yuan et al., 2009). The linear equation was fitted as $y = -0.1681 \times \lg(x) + 0.4277$ (x: nM) with a correlation coefficients of 0.9883. Furthermore, the colorimetric biosensor was found to show very desirable reproducibility due to its homogeneous assay format. The relative standard deviations (RSDs) of peak absorbance readings were 1.5%, 2.3%, 1.0%, 1.1% and 2.1% in four repetitive assays of 5 pM, 15 pM, 80 pM, 2 nM, and 25 nM PI3K. Therefore, we might conclude that the developed method held great potential for quantitative activity assay of PI3K with desirable sensitivity and reproducibility.

3.4. Assay activity screening of PI3K in cells using the Biosensing Strategy

The feasibility of the developed biosensor in assay of real complex biological samples was explored. We measured the PI3K activity in different cell extracts including the human breast cancer cell lines (MCF-7), cervical cancer cell lines (Hela), and breast cancer cell lines (MDA-MB-231). The expression levels of PI3K in these three cell lysates were determined using the proposed biosensing method with reference to a commercial PI3K assay kit. The data indicated that the developed method gave comparable results with the commercialized kit (Fig. S3). These results suggested that the proposed method held the promise for sensitive detection of PI3K in real complex samples.

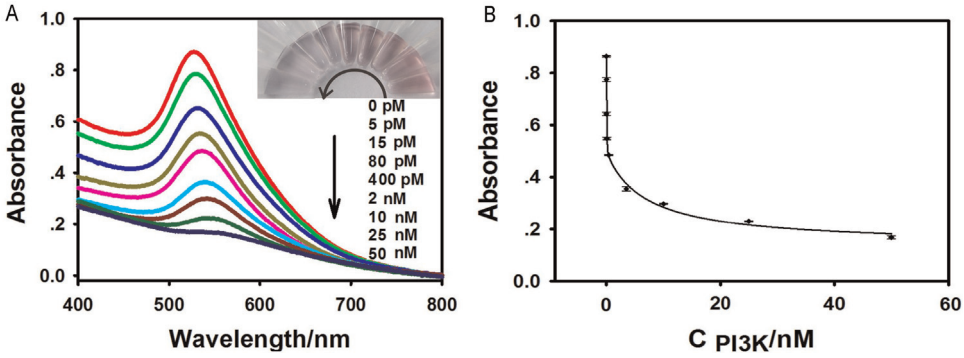

Fig. 4. (A) Typical absorption spectral responses of the biosensor to PI3K of varying concentrations. Inset: photograph of the corresponding solutions. (B) Absorption peak intensities at 526 nm obtained by the biosensor versus PI3K concentrations. Error bars indicated SDs across four repetitive assays. (For interpretation of the references to color in this figure, the reader is referred to the web version of this article.)

3.5. Enzyme-activated Colorimetric Biosensing Strategy for PTEN assay

To demonstrate the utility of the strategy for detecting other phosphoinositide enzymes, we investigated the implementation of the biosensor for PTEN-mediated signaling assay. PTEN regulates the PIP3 level in cell membrane by reversing the action of PI3K. To construct the biosensor for PTEN, we utilized DMPC, MHPC and PIP3 to engineer the AuNP supported artificial cell membranes, and still used the AuNPs modified with PIP3 binding PH domains for PTEN-inactivated assembly of AuNPs, as illustrated in Scheme 3. In the absence of PTEN, the PH domain modified AuNPs could bind to PIP3 that incorporated in the phospholipid membranes on the surface of AuNPs, and thus induce a cross-linked assembly of AuNPs. In the presence of PTEN, the phosphate group at the D-3 position of the inositol ring of PIP3 was removed by PTEN to generate PIP2. Since the interaction of the PH domain is specific to PIP3, the cross-linked assembly of AuNPs between the PH domain modified AuNPs and the phospholipid membrane coated AuNPs was inactivated. Hence, the inactivated assembly of AuNPs gave a quantitative measure for the detection of the PTEN-catalyzed dephosphorylation activity.

Typical absorption spectral responses and photographs in the PTEN assay were shown in Fig. 5A. After the addition of PIP3 binding PH domain modified AuNPs in a solution containing AuNP supported phospholipids membranes not incorporating PIP3, the mixture displayed a red color with a remarkable absorption peak to 526 nm (Fig. 5A, curve a). In contrast, after the addition of PIP3 binding PH domain modified AuNPs, the solution of PIP3-incoporated phospholipid-coated AuNPs gave a substantially decreased absorption peak with the absorption peak shifted to 550 nm (Fig. 5A, curve d). These observations implied that the aggregation of the phospholipid-coated AuNPs with the PH domain modified AuNPs was specific to the interaction between PIP3 and its binding domain. On the other hand, there was no appreciable spectral change for the AuNPs solution after the phospholipid-coated AuNPs incubated with 18 nM PTEN followed by the addition of the PH domain modified AuNPs (Fig. 5A, curve b). This finding revealed that the reaction of PIP3-incoporated phospholipid-coated AuNPs with PTEN could prevent their cross-linked assembly with the PIP3 binding PH domain modified AuNPs, suggesting the PTEN-mediated removal of PIP3 from the phospholipid-coated AuNPs. In addition, when the phospholipid-coated AuNPs were incubated with PTEN in the presence of a PTEN inhibitor, SF1670 (100 μM), followed by the addition of the PH domain modified AuNPs, a significant absorption peak decrease was obtained for the reaction mixture (Fig. 5A, curve c). This finding implied that the prevention of the assembly of PIP3-incoporated phospholipid-coated AuNPs and PIP3 binding PH domain modified AuNPs was specific to an active PTEN reaction. The visual observations of the color changes were also in good agreement with these spectral measurements, implying that the biosensor could be used for the detection of PTEN signaling.

The biosensor was also capable of quantifying the PTEN activity, as shown in Fig. 5B. In the assays with PTEN of varying concentrations, the absorption peaks were observed to increase in dynamic correlation to increasing PTEN concentrations in the range from 10 pM to 18 nM with a concomitant blue-shift from 550 nm to 526 nm. The absorbance readings at 526 nm exhibited a linear correlation to the logarithmic PTEN concentrations in this range (Fig. S4). The linear equation was fitted as $y=0.1208\times \lg(x)+0.3897$ (x: pM) with a correlation coefficients of 0.9872. The readily achieved detection limit was 2 pM. Such a low detection limit was much better (at least 10-fold improvement) than existing methods for PTEN assays (Taniguchi et al., 2006; Tzenaki et al., 2012), implying the potential of the biosensor for sensitive detection of PTEN activity.

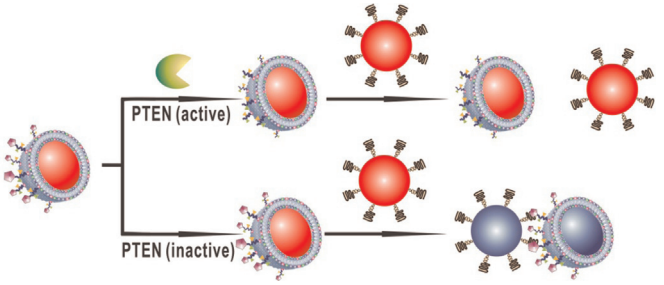

Scheme 3. Illustration of biosensor strategy for PTEN via enzymatic inactivated assembly of AuNP supported PIP3-incorporated phospholipid membranes with PIP3 binding PH domain modified AuNPs.

4. Conclusions

In conclusion, we have developed a novel enzyme-activated AuNPs assembly strategy as a homogeneous colorimetric biosensor for activity detection of phosphoinositide kinases and phosphatases. This strategy utilizes a biomimetic mechanism of phosphoinositide signaling, in which AuNP supported phospholipid membranes were constructed to mimic the cellular membrane substrate, and AuNP modified binding PH domain was designed for specific recognition of the phosphorylated phosphoinositides. The biomimetic strategy enables efficient enzymatic reactions of the substrate and highly selective detection of the target enzyme

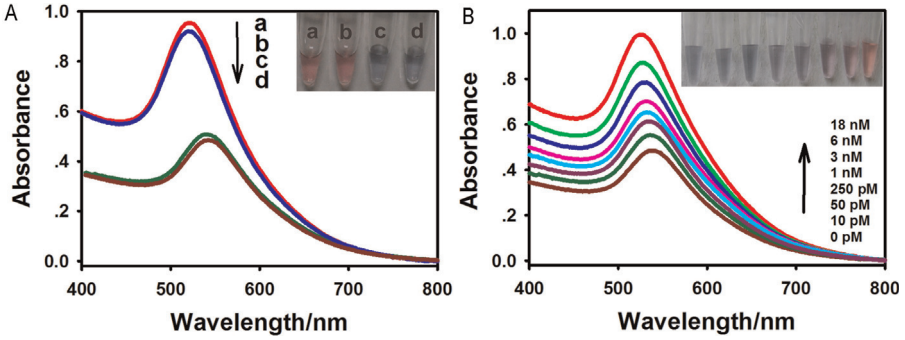

Fig. 5. (A) Absorption spectral responses of the biosensor in the assay of PTEN. (a) PIP3-free phospholipid-coated AuNPs+PH domain modified AuNPs; (b) PIP3-incorporated phospholipid-coated AuNPs+18 nM PTEN+PH domain modified AuNPs; (c) PIP3-incorporated phospholipid-coated AuNPs+18 nM PTEN+inhibitor SF1670 (100 μM)+PH domain modified AuNPs; (d) PIP3-incorporated phospholipid-coated AuNPs+PH domain modified AuNPs. Inset: photograph of the corresponding solutions. (B) Absorption spectral responses of the biosensor to PTEN of varying concentrations. Inset: photograph of the corresponding solutions. (For interpretation of the references to color in this figure, the reader is referred to the web version of this article).

with minimized interference. The developed biosensor strategy allows convenient, rapid, sensitive visual detection of phosphoinositide enzymes with a pM detection limit and a four-decade wide dynamic range. The biosensor is also demonstrated for the utility for enzyme assay in real cell lysate samples. Moreover, the biosensor is configured into a homogeneous format that increases the potential for high-throughput analysis. In view of these advantages, the developed strategy might create a general biosensor platform for visual detection of phosphoinositide signaling with high sensitivity and selectivity in biomedical research and clinical diagnostics.

Acknowledgments

This work was supported by NSFC, China (21025521, 21205034, 21035001, 21190041, and 91317312), National Key Basic Research Program, China (2011CB911000), European Commission FP7-HEALTH-2010 Programme-GlycoHIT (260600), Doctoral Fund of Ministry of Education of China (New Teachers, 20120161120032), and Hunan Provincial NSFC, China (13JJ4031).

Appendix A. Suplementary information

Supplementary data associated with this article can be found in the online version at http://dx.doi.org/10.1016/j.bios.2014.06.016.

References

Bartel, D.P., 2004. Cell 116, 281–297.
Bunney, T.D., Katan, M., 2010. Nat. Rev. Cancer 10, 342–352.
Bethoney, K.A., King, M.C., Hinshaw, J.E., Ostap, E.M., Lemmon, M.A., 2009. Proc. Natl. Acad. Sci. USA 106, 13359–13364.
Chen, Z., Tan, Y., Zhang, C., Yin, L., Ma, H., Ye, N., Lin, Y., 2014. Biosens. Bioelectron. 56, 46–50.
Cantley, L.C., 2002. Science 296, 1655–1657.
Cully, M., You, H., Levine, A.J., Mak, T.W., 2006. Nat. Rev. Cancer 6, 184–192.
Giljohann, D.A., Seferos, D.S., Daniel, W.L., Massich, M.D., Patel, P.C., Mirkin, C.A., 2010. Angew. Chem. Int. Ed. 49, 3280–3294.
Guo, Y., Wang, Z., Qu, W., Shao, H., Jiang, X., 2011. Biosens. Bioelectron. 26, 4064–4069.
Hill, H.D., Mirkin, C.A., 2006. Nat. Protoc. 1, 324–336.
Ip, S., MacLaughlin, C.M., Gunari, N., Walker, G.C., 2011. Langmuir 27, 7024–7033.
Knight, Z.A., Feldman, M.E., Balla, A., Balla, T., Shokat, M., K., 2007. Nat. Protoc. 2, 2459–2466.
Liu, S.J., Wen, Q., Tang, L.J., Jiang, J.H., 2012. Anal. Chem. 84, 5944–5950.
Li, L.L., Zhang, R., Yin, L., Zheng, K., Qin, W., Selvin, P.R., Lu, Y., 2012a. Angew. Chem. Int. Ed. 124, 6225–6229.
Li, J., Fu, H.E., Wu, L.J., Zheng, A.X., Chen, G.N., Yang, H.H., 2012b. Anal. Chem. 84, 5309–5315.
Lemmon, M.A., 2008. Nat. Rev. Mol. Cell Biol. 9, 99–111.
Li, Y., Prasad, A., Jia, Y., Roy, S.G., Loison, F., Mondal, S., Luo, H.R., 2011. Blood 117, 6702–6713.
Martelli, A.M., Nyåkern, M., Tabellini, G., Bortul, R., Tazzari, P.L., Evangelisti, C., Cocco, L., 2006. Leukemia 20, 911–928.
Nie, H.G., Liu, S.J., Yu, R.Q., Jiang, J.H., 2009. Angew. Chem. Int. Ed. 48, 1–6.
Pornpattananangkul, D., Zhang, L., Olson, S., Aryal, S., Obonyo, M., Vecchio, K., Zhang, L., 2011. J. Am. Chem. Soc. 133, 4132–4139.
Qian, X., Peng, X.H., Ansari, D.O., Yin-Goen, Q., Chen, G.Z., Shin, D.M., Nie, S., 2008. Nat. Biotechnol. 26, 83–90.
Saha, K., Agasti, S.S., Kim, C., Li, X., Rotello, V.M., 2012. Chem. Rev. 112, 2739–2779.
Taniguchi, C.M., Tran, T.T., Kondo, T., Luo, J., Ueki, K., Cantley, L.C., Kahn, C.R., 2006. Proc. Natl. Acad. Sci. USA 103, 12093–12097.
Tzenaki, N., Andreou, M., Stratigi, K., Vergetaki, A., Makrigiannakis, A., Vanhaesebroeck, B., Papakonstanti, E.A., 2012. FASEB J 26, 2498–2508.
Thaxton, C.S., Daniel, W.L., Giljohann, D.A., Thomas, A.D., Mirkin, C.A., 2009. J. Am. Chem. Soc. 131, 1384–1385.
Tam, N.C., Scott, B.M., Voicu, D., Wilson, B.C., Zheng, G., 2010. Bioconjugate Chem. 21, 2178–2182.
Tam, N.C., McVeigh, P.Z., MacDonald, T.D., Farhadi, A., Wilson, B.C., Zheng, G., 2012. Bioconjugate Chem. 23, 1726–1730.
Wymann, M.P., Schneiter, R., 2008. Nat. Rev. Mol. Cell Biol. 9, 162–176.
Wei, Y., Jiang, Y., Zou, F., Liu, Y., Wang, S., Xu, N., Jiang, J., 2013. Proc. Natl. Acad. Sci. USA 110, 6829–6834.
Wang, L.S., Wu, L.C., Lu, S.Y., Chang, L.L., Teng, I.T., Yang, C.M., Ho, J.A.A., 2010. ACS Nano 4, 4371–4379.
Yuan, H.T., Khankin, E.V., Karumanchi, S.A., Parikh, S.M., 2009. Mol. Cell Biol. 29, 2011–2022.
Zheng, W., Liu, Y., West, A., Schuler, E.E., Yehl, K., Dyer, R.B., Salaita, K., 2014. J. Am. Chem. Soc. 136, 1992–1999.
Zhang, X., Servos, M.R., Liu, J., 2012. J. Am. Chem. Soc. 134, 7266–7269.